



# Ultrasound-assisted dissolution of cellulose in ionic liquid

Wu Lan<sup>a</sup>, Chuan-Fu Liu<sup>a,\*</sup>, Feng-Xia Yue<sup>a</sup>, Run-Cang Sun<sup>a,b</sup>, John F. Kennedy<sup>c</sup>

<sup>a</sup> State Key Laboratory of Pulp and Paper Engineering, South China University of Technology, Guangzhou 510640, China

<sup>b</sup> College of Material Science and Technology, Beijing Forestry University, Beijing 100083, China

<sup>c</sup> Birmingham Carbohydrate and Protein Technology Group, School of Chemistry, University of Birmingham, Birmingham B15 2TT, UK

## ARTICLE INFO

### Article history:

Received 22 July 2010

Received in revised form 4 May 2011

Accepted 11 May 2011

Available online 18 May 2011

### Keywords:

Cellulose

Ultrasound irradiation

Dissolution

Ionic liquid

## ABSTRACT

Ultrasound-assisted dissolution of cellulose was performed in ionic liquid 1-butyl-3-methylimidazolium chloride ([C<sub>4</sub>mim]Cl). The dissolution process was monitored with polarizing microscope. The effects of parameters including ultrasonic power and irradiation time on cellulose dissolution time were investigated. The dissolution time required for complete dissolution decreased from 190 min without assistance to 60 min irradiated with 30 W ultrasound for 20 min. The regenerated cellulose samples were characterized with FT-IR, solid-state CP/MAS <sup>13</sup>C NMR, wide-angle X-ray diffraction and thermal analysis. The results showed that most crystalline structure of cellulose was destroyed to amorphous structure, and the remained crystalline structure of cellulose was converted to cellulose II from cellulose I in native cellulose. After dissolution and regeneration in ionic liquid, the thermal stability of cellulose decreased and the pyrolysis residues increased.

© 2011 Elsevier Ltd. All rights reserved.

## 1. Introduction

Due to the stiff molecules and close chain packing via the numerous inter- and intra-molecular hydrogen bonds, it is extremely hard to dissolve cellulose in water and in most common organic solvents, which constitutes a major obstacle for cellulose application. The solvents for efficient cellulose dissolution have been searched for since the confirmation of cellulose molecules. To date, a number of solvent systems, such as inorganic molten salts like LiClO<sub>4</sub>·3H<sub>2</sub>O (Fischer, Leipner, Thummler, Brendler, & Peters, 2003), *N*-methylmorpholine-*N*-oxide (NMMO) (Rosenau, Hofinger, Potthast, & Kosma, 2003), DMAc/LiCl (Araki et al., 2006), DMF/N<sub>2</sub>O<sub>4</sub> (Philipp, Nehls, & Wagenknecht, 1987), and DMSO/TBAF (Ramos, Frollini, & Heinze, 2005), have been found efficient for cellulose dissolution. However, there remain limitations such as toxicity, cost, difficulty in solvent recovery, or instability in processing.

Recently, due to their unique physico-chemical properties, such as chemical and thermal stability, non-flammability and immeasurably low vapor pressure, ionic liquids have been considered as the most potential green solvents in the future, which have attracted a great deal of scientific attention in many fields (Forsyth, MacFarlane, Thomson, & von Itzstein, 2002; Turner, Spear, Huddleston, Holbrey, & Rogers, 2003). Many kinds of ionic liquids with a variety of structures have been reported as novel solvents for cellulose dissolution, such as a series of alkylimidazolium salts con-

taining chloride (Heinze, Schwikal, & Barthel, 2005; Luo, Li, & Zhou, 2005; Swatloski, Spear, Holbrey, & Rogers, 2002; Zhang, Wu, Zhang, & He, 2005), formate (Fukaya, Sugimoto, & Ohno, 2006), acetate (de Maria & Martinsson, 2009; Hermanutz, Gaehr, Uerdingen, Meister, & Kosan, 2007; Kosan, Michels, & Meister, 2008), and alkylphosphate (Fukaya, Hayashi, Wada, & Ohno, 2008; Kamiya et al., 2008; Mazza, Catana, Vaca-Garcia, & Cecutti, 2009). In addition, the dissolution of other biopolymers such as hemicelluloses (Ren, Sun, Liu, Cao, & Luo, 2007), lignin (Pu, Jiang, & Ragauskas, 2007), starch (Biswas, Shogren, Stevenson, Willett, & Bhowmik, 2006), chitosan (Xie, Zhang, & Li, 2006), protein (Biswas et al., 2006), and wood (Fort et al., 2007; Kilpelainen et al., 2007) in ionic liquids has also been reported over the last few years, indicating the potential utilization of ionic liquids in the field of biopolymer chemistry.

Ionic liquids have been focused as solvents and reaction media for cellulose processing and derivatization to produce novel materials, among which the most common ionic liquid is 1-butyl-3-methylimidazolium chloride ([C<sub>4</sub>mim]Cl). However, it was reported that 10 h dissolution time was needed for complete dissolution of cellulose in [C<sub>4</sub>mim]Cl (Heinze et al., 2005). It is too long for cellulose processing and derivatization to produce materials both in laboratory and industrial scale.

Ultrasonic treatment is well established in the separation of plant materials, particularly for extraction of low molecular weight substances. The mechanical and chemical effects of ultrasound are believed to accelerate the extraction of organic compounds from plant materials due to disruption of cell walls and enhanced mass transfer of the cell wall contents (Aliyu & Hepher, 2000). The purpose of the present work was to investigate whether ultrasound

\* Corresponding author. Tel.: +86 20 87111861; fax: +86 20 87111861.  
E-mail address: [chfliu@gmail.com](mailto:chfliu@gmail.com) (C.-F. Liu).

irradiation is capable of enhancing cellulose dissolution in ionic liquid and its effect on physicochemical properties of regenerated cellulose.

## 2. Experimental

### 2.1. Materials

Sugarcane bagasse was obtained from a local sugar factory (Guangzhou, China). It was dried in sunlight and then cut into small pieces. The cut SCB was ground and screened to prepare 40–60 mesh size particles. The ground SCB was dried again in a cabinet oven with air circulation for 16 h at 50 °C.

Ionic liquid [C<sub>4</sub>mim]Cl, 1-butyl-3-methylimidazolium chloride, was purchased from the Chemer Chemical Co., Ltd., Hangzhou, China, and used as received. All of other chemicals used were of analytical grade and obtained from Guangzhou Chemical Reagent Factory, China.

### 2.2. Isolation of cellulose from sugarcane bagasse

The dried and ground SCB powder was firstly dewaxed in acetone at 20 °C for 16 h. The dewaxed SCB was oven-dried and then delignified with 6% sodium chlorite at pH 3.8–4.0, adjusted by acetic acid, for 2 h at 75 °C. The residues were collected by filtration and washed thoroughly with distilled water until the filtrate was neutral. Then it was washed with ethanol and dried in a cabinet oven at 55 °C for 16 h. To release the hemicelluloses, the holocellulose obtained was extracted with 10% KOH at 20 °C for 10 h with a solid to extractant ratio of 1:20 (g/mL). After filtration, the cellulosic residues were washed thoroughly with distilled water until the filtrate was neutral. In order to improve dissolution efficiency in ionic liquid, the obtained samples were suspended in 95% ethanol for 10 h to remove the water present in cellulose. After filtration, the residues were dried in an oven at 55 °C for 16 h.

### 2.3. Dissolution and regeneration of cellulose

Dried cellulose was added into a flask containing [C<sub>4</sub>mim]Cl with a weight ratio of 2% (cellulose to [C<sub>4</sub>mim]Cl). The flask was continuously purged with gaseous N<sub>2</sub>, and the mixture of cellulose/[C<sub>4</sub>mim]Cl was stirred in an oil bath at 110 °C for 5 min to guarantee the melting of [C<sub>4</sub>mim]Cl and the wetting of cellulose with [C<sub>4</sub>mim]Cl. Then the mixture was irradiated at 110 °C for 0, 5, 10, 15, and 20 min, respectively, with ultrasound provided with a horn at sonic power of 20, 30, 40, 50, 60 and 75 W, respectively. After ultrasound irradiation, the mixture was stirred at 110 °C until the cellulose was completely dissolved. The dissolution process was monitored with polarizing microscope. After the complete dissolution of cellulose in [C<sub>4</sub>mim]Cl, the resulting mixture was slowly poured into 250 mL ethanol with vigorous agitation. The solid deposits were collected by filtration, washed thoroughly with ethanol to eliminate [C<sub>4</sub>mim]Cl, and then freeze-dried. The yield was determined from the regenerated cellulose on the basis of initial oven-dried measurements. To reduce errors and confirm the results, all experiments were performed at least in duplicate, and the yield represents the average value.

### 2.4. Recycling of ionic liquid

The liquors containing [C<sub>4</sub>mim]Cl and ethanol, obtained from cellulose regeneration, were mixed and concentrated under reduced pressure. Then the concentrated solution was freeze-dried over 48 h to obtain the recycled [C<sub>4</sub>mim]Cl.

### 2.5. Characterization of the native and regenerated cellulose

The neutral sugar composition of the native cellulose obtained from sugarcane bagasse was determined by gas chromatography (GC) analysis of the corresponding alditol acetates. The sample (10 mg) was treated with 72% H<sub>2</sub>SO<sub>4</sub> (0.125 mL) for 45 min at room temperature by agitation on a vortex mixture. The solution was then diluted to 1.475 mL, heated to 100 °C for 2.5 h, cooled, and neutralized with 0.32 mL of 15 M ammonia. After reduction, the resulting alditols were acetylated for GC analysis as described by Blakeney, Harris, Henry, and Stone (1983).

Viscosity of native and regenerated cellulose was measured by British Standard Methods for determination of limiting viscosity number of cellulose in dilute solutions, Part 1 cupriethylenediamine (CED) method (BS 6306, Part 1, 1982). The viscosity average DP (degree of polymerization) of cellulose was estimated from its intrinsic viscosity  $[\eta]$  in CED hydroxide solution,  $P^{0.90} = 1.65[\eta]$ , where  $P$  is an indeterminate average DP (Evans & Wallis, 1989). Molecular weight (Mw) of cellulose was then calculated from  $P$  by multiplied by 162, the Mw of an AGU.

The FT-IR spectra of the native and regenerated cellulose were recorded on an FT-IR spectrophotometer (Nicolet 510) from finely ground samples (1%) in KBr pellets in the range 4000–400 cm<sup>-1</sup>. Thirty-two scans were taken for each sample with a resolution of 2 cm<sup>-1</sup> in the transmission mode.

The solid-state CP/MAS <sup>13</sup>C NMR spectra were obtained on a Bruker DRX-400 spectrometer with 5 mm MAS BBO probe employing both Cross Polarization and Magic Angle Spinning and each experiment was recorded at ambient temperature. The spectrometer operated at 100 MHz. Acquisition time was 0.034 s, the delay time 2 s, and the proton 90° pulse time 4.85 μs. Each spectrum was obtained with an accumulation of 5000 scans.

The wide-angle X-ray diffraction pattern of the native and regenerated cellulose was recorded on a Rigaku (Japan) D/MAX-III A X-ray diffractometer equipped with Ni-filtered Cu Kα<sub>1</sub> radiation ( $\lambda = 0.154$  nm) at room temperature. The operating voltage and current were 40 kV and 30 mA, respectively. The scattering angle range was from 5° to 45° with 8°/min scanning speed and a 2 $\theta$  step interval of 0.02°.

Thermal analysis of the native and regenerated cellulose was performed using thermogravimetric analysis (TGA) on a thermal analyzer (SDT Q500, TA Instrument). The apparatus was continually flushed with nitrogen. The sample weighed between 7 and 11 mg and the scans were run from room temperature to 600 °C at a rate of 10 °C/min.

## 3. Results and discussion

### 3.1. Dissolution and regeneration of cellulose

Delignification of dewaxed bagasse followed by alkaline extraction yielded 49.5% cellulose (based on the dry weight of sugarcane bagasse). The neutral sugar composition of the obtained cellulose showed that glucose was the predominant sugar component, which comprised 94.5% of the total sugars, indicating a relatively high content of cellulose. Small amounts of non-cellulosic sugars, such as xylose (2.8%), galactose (1.7%), mannose (0.9%), and arabinose (0.6%), were also observed, indicating the presence of minor quantities of residual hemicelluloses in the cellulosic preparation. The intrinsic viscosity, degree of polymerization, and molecular weight of the native cellulosic preparation were determined to be 378 mL g<sup>-1</sup>, 1277, and 206 800 g mol<sup>-1</sup>, respectively.

The dissolution of cellulose in the ionic liquid [C<sub>4</sub>mim]Cl assisted by ultrasonic irradiation were studied. The polarizing microscope was employed to monitor the variation of the cellulose during the

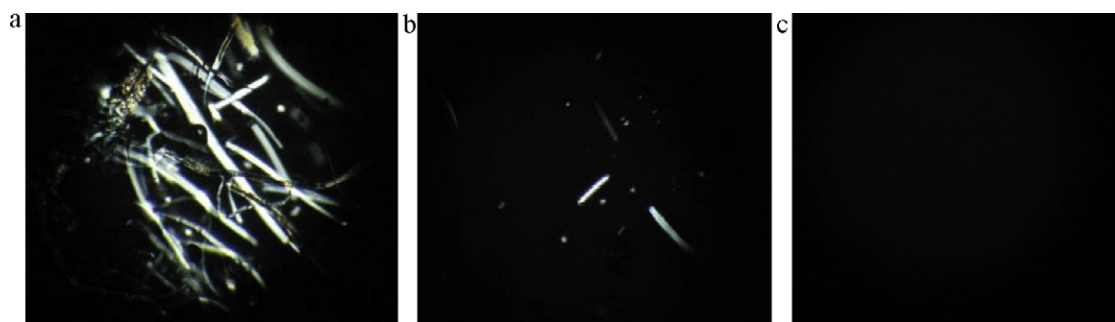


**Fig. 1.** PLM images of cellulose dissolved in [C<sub>4</sub>mim]Cl at 110 °C for 0 min (a), 10 min following irradiation with 60 W ultrasound for 10 min (b), and 100 min following irradiation with 60 W ultrasound for 10 min (c).

dissolution process to determine the complete dissolution of cellulose in [C<sub>4</sub>mim]Cl. The dissolution process under the polarizing microscope is shown in Fig. 1. It could be seen that at the beginning of [C<sub>4</sub>mim]Cl treatment, there was bright eyeshot (Fig. 1a) under the polarizing microscope, which was due to the presence of extensive crystalline structure in initial native cellulose. As the dissolution time increased, the eyeshot of the microscope turned gloomy. Fig. 1b shows the viewing field of the cellulose suspension obtained after irradiation for 10 min with 60 W ultrasound followed by agitation at 110 °C for 10 min. Most cellulose was dissolved and there were only small amounts of crystalline cellulose particles remained. After stirring for 100 min following ultrasonic irradiation, cellulose was completely dissolved and the eyeshot of the polarizing microscope became black, as shown in Fig. 1c.

Table 1 lists the dissolution and regeneration of cellulose in the [C<sub>4</sub>mim]Cl assisted with ultrasound irradiation. As shown in Table 1, the yield of regenerated cellulosic samples was between 97% and 105%. The reduced weight was primarily due to the weight loss during cellulose regeneration processes, including washing and transferring. The weight gain was probably due to the impurities involved in regenerated cellulose.

It was obvious that ultrasound irradiation had beneficial effect on cellulose dissolution. The increment of ultrasound irradiation time from 0 (sample 1) to 5 (sample 2), 10 (sample 3), 15 (sample 4), and 20 min (sample 5) led to the decrease in cellulose dissolution time from 190 to 150, 120, 100, and 60 min, which was probably due that ultrasound irradiation provided a greater penetration of ionic liquid into cellulose and improved mass transfer. When the dissolving system was irradiated with ultrasound, the extreme condition was probably obtained. It was said that transient temperature of at least 5000 K and pressure up to 1200 bar could be achieved (Adewuyi, 2001; Kardos & Luche, 2001), accompanied by

vigorously physical agitation and shock. All of the abovementioned effects provided excellent conditions for cellulose dissolution in ionic liquid. This beneficial effect of ultrasound techniques has also been reported in isolation of cell wall polymers (Aliyu & Hepher, 2000). Cellulose dissolution time decreased from 147 (sample 6) to 120 (sample 3), 110 (sample 7) and 100 min (sample 8) with the improvement of ultrasonic power from 20 to 30, 40 and 50 W. However, further improvement of ultrasonic power (samples 8–10) did not result in the decrement in cellulose dissolution time. Compared with sample 3 obtained with one-step ultrasound irradiation, 120 min of dissolution time was also needed for sample 11 with two-step irradiation with 5 min interval, indicating that the same ultrasound energy obtained from same power and total irradiation duration did not result in different effect on cellulose dissolution.

DP of native and regenerated cellulose is listed in Table 1. After dissolution and regeneration, DP decreased from 1263 for native cellulose to 945 for regenerated cellulose sample obtained without ultrasound irradiation. Ultrasound irradiation for 5, 10, 15, and 20 min led to a slight reduction of DP to 799, 800, 744 and 682, respectively. However, the increase of ultrasound power from 20 to 40, 50, and 75 W resulted in an improvement of DP from 946 to 962, 1022, and 1019. The reason for this improvement is not clear and probably due to the reassociation and polymerisation of the radicals formed at higher ultrasound power.

In present study, we also recycled ionic liquid [C<sub>4</sub>mim]Cl after simply removing ethanol and freeze-drying. Similar data were obtained when the recycled [C<sub>4</sub>mim]Cl was used (sample 12). The satisfactory results were also reported on wood dissolution and acetylation in recycled [C<sub>4</sub>mim]Cl compared with those in fresh [C<sub>4</sub>mim]Cl (Xie, King, Kilpelainen, Granstrom, & Argyropoulos, 2007).

**Table 1**  
Dissolution and regeneration of cellulose in [C<sub>4</sub>mim]Cl assisted with ultrasound irradiation.

Dissolution conditions			Dissolution and regeneration			
Ultrasonic power (W)	Irradiation time (min) <sup>a</sup>	Temperature (°C)	Sample no.	Dissolution time (min)	Yield (%)	DP
30	0	110	1	190	99	945
30	5	110	2	150	100	799
30	10	110	3	120	100	800
30	15	110	4	100	101	744
30	20	110	5	60	101	682
20	10	110	6	147	98	946
40	10	110	7	110	99	962
50	10	110	8	100	97	1022
60	10	110	9	100	101	–
75	10	110	10	99	105	1019
30	10	110	11	120	104	–
30	10	110	12 <sup>b</sup>	118	101	814

<sup>a</sup> Samples 1–10 were obtained with one-step ultrasound irradiation, while sample 11 was irradiated at 110 °C for 5 min, stirred for 5 min in interval, and irradiated for another 5 min.

<sup>b</sup> Using recycled [C<sub>4</sub>mim]Cl as the solvent.

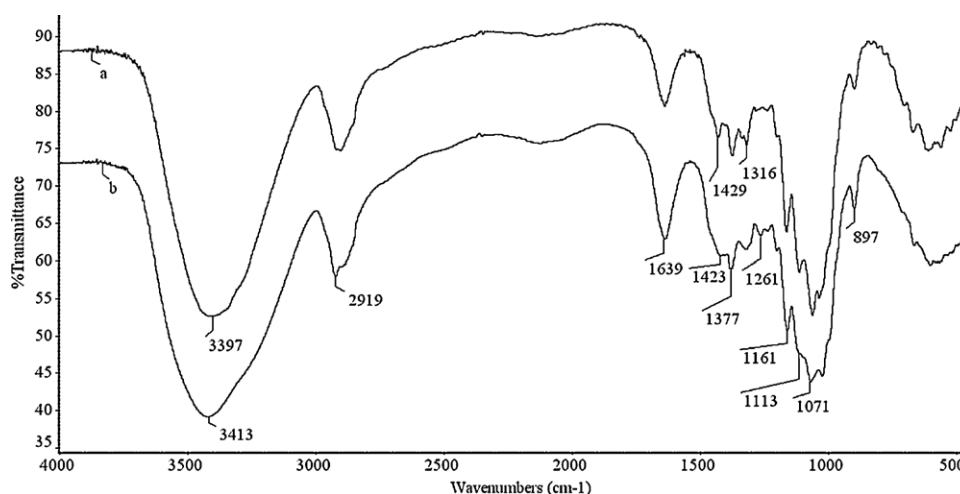


Fig. 2. FT-IR spectra of native cellulose (spectrum a) and regenerated cellulose obtained after dissolution without ultrasound irradiation (spectrum b, sample 6).

### 3.2. FT-IR spectra

Common methods for the characterization of cellulose structure are based on X-ray, infrared (IR) absorption, and NMR. Among them, wide-angle X-ray diffraction gives the most direct results and quantitative information. FT-IR and NMR spectroscopy show some useful information related to the change of hydrogen bonding during crystal transformation (Oh et al., 2005). The aim of using FT-IR in present study is to measure the changes of the structure of the regenerated cellulose samples obtained after dissolution in ionic liquid assisted with or without ultrasound irradiation. Fig. 2 illustrates FT-IR spectra of native cellulose (spectrum a) and regenerated cellulose (spectrum b, sample 6). Evidently, the bands in the two spectra are rather similar, indicating the similar structure of native cellulose and regenerated cellulose, which suggested that ionic liquid was a direct solvent of cellulose. In spectrum a, the absorption at  $3397\text{ cm}^{-1}$  is attributed to the O–H stretching and that of  $2919\text{ cm}^{-1}$  is attributed to the C–H stretching. A small peak at  $1429\text{ cm}^{-1}$  relates to the  $\text{CH}_2$  symmetric bending. The absorbances at  $1377$ ,  $1316$ , and  $1261\text{ cm}^{-1}$  originate from the O–H bending, C–H bending, and C–O symmetric stretching (Liu et al., 2007b; Sun, Sun, Tomkinson, & Baird, 2004). The peak at  $1161\text{ cm}^{-1}$  arises from C–O anti-symmetric stretching (Liu, Zhang, Li, Yue, & Sun, 2010). A shoulder band at  $1113\text{ cm}^{-1}$  belongs to C–OH skeletal vibration. The C–O–C pyranose ring skeletal vibration gives a prominent band at  $1071\text{ cm}^{-1}$ . A small sharp peak at  $897\text{ cm}^{-1}$  corresponds to the glycosidic C<sub>1</sub>–H deformation with ring vibration contribution, which is characteristic of  $\beta$ -glycosidic linkages between glucose in cellulose. The band at  $1639\text{ cm}^{-1}$  is due to the bending mode of the absorbed water. Significantly, the disappearance of the band at  $1520\text{ cm}^{-1}$  revealed that the cellulose isolated from bagasse was free of residual lignin.

Compared with spectrum a, there were small differences of absorbances in spectrum b. The absorption from O–H stretching vibration shifted from  $3397\text{ cm}^{-1}$  in spectrum a to  $3413\text{ cm}^{-1}$  in spectrum b, indicating the content of free hydroxyl group without cross-linking to form hydrogen bonds increased in regenerated cellulose. The peak of the  $\text{CH}_2$  bending shifted from  $1429\text{ cm}^{-1}$  in spectrum 1 to  $1423\text{ cm}^{-1}$  in spectrum b, which was a hint of the cleavage of hydrogen bond in C<sub>6</sub>–OH to some extent (Zhang et al., 2005).

The spectra of regenerated cellulose samples after dissolution in ionic liquid with or without ultrasound irradiation were similar except that of sample 10 (spectrum not shown), which gives a peak at  $1574\text{ cm}^{-1}$  from anti-symmetric stretching of carboxylic anions.

It was suggested that carboxyl groups were formed during dissolution and regeneration, which indicated that the irradiation of ultrasound with relatively high power resulted in oxidative degradation of cellulose (Liu et al., 2007a).

The intensity ratio of absorbance for O–H bending and C–H stretching in FT-IR spectra of cellulose can be used to reflect the relative changes of cellulose crystallinity. In present study, N.O'KI of regenerated cellulose was calculated from FT-IR, and the results are listed in Table 2. As seen in Table 2, the N.O'KI of regenerated cellulose increased from 0.930 to 0.963 and 1.084 with the improvement of irradiation time from 0 to 5 and 10 min. However, further enhancement of ultrasonic irradiation time from 10 to 15 and 20 min resulted in a decrease in N.O'KI from 1.084 to 0.975 and 0.966. However, a clear trend of N.O'KI of regenerated cellulose was not found with the enhancement of ultrasonic power, and the reason need to be further studied.

### 3.3. Solid-state CP/MAS $^{13}\text{C}$ NMR spectra

Fig. 3 shows the CP/MAS  $^{13}\text{C}$  NMR spectra of native cellulose (spectrum a) and regenerated cellulose samples 1 (spectrum b) and 4 (spectrum c). It can be seen that the all noticeable signals in spectrum a are distributed in the region between 60 and 110 ppm for the carbon atoms of cellulose. The signals at 105.8 ppm (C-1), 89.7 ppm (C-4 of crystalline cellulose), 85.4 ppm (C-4 of amorphous cellulose), 75.8 (C-2 and C-3, and C-5), 65.9 (C-6 of crystalline cellulose) and 63.3 ppm (C-6 of amorphous cellulose) have all been reported before (Bardet, Foray, & Tran, 2002; Chang & Chang, 2001; Maunu, 2002). Apparently, there are differences between spectra of regen-

Table 2

Relative changes of crystallinity of native and regenerated cellulose calculated from FT-IR spectra.

Sample no.	C–H stretching	O–H bending	N.O'KI
1	0.271	0.252	0.930
2	0.190	0.183	0.963
3	0.154	0.167	1.084
4	0.151	0.147	0.974
5	0.238	0.230	0.966
6	0.107	0.116	1.084
7	0.145	0.139	0.959
8	0.144	0.150	1.042
9	0.180	0.168	0.933
10	0.279	0.290	1.039
11	0.134	0.132	0.985
12	0.172	0.182	1.058



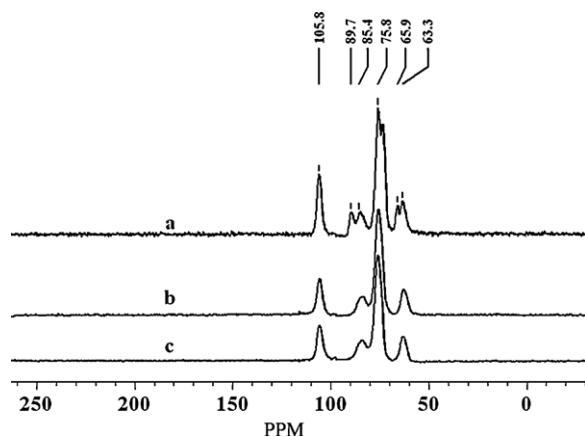


Fig. 3. CP/MAS  $^{13}\text{C}$  NMR spectra of native cellulose (spectrum a) and regenerated cellulose samples 1 (spectrum b) and 4 (spectrum c).

erated cellulose and that of native cellulose. In spectra b and c, the signals at 89.7 ppm for C-4 of crystalline cellulose and 65.9 ppm for C-6 of crystalline cellulose disappeared, indicating that the crystalline structure in native cellulose was destroyed and amorphous cellulose was obtained. These suggested that the regenerated cellulose was mainly composed of amorphous structure, corresponding to the increased content of free hydroxyl groups obtained from FT-IR analysis. In addition, compared with spectrum a, there were no new signals present in spectra b and c, indicating no chemical reaction occurred during dissolution assisted with ultrasound irradiation, which is accordance with the results from FT-IR.

### 3.4. Wide-angle X-ray diffraction

Fig. 4 illustrates the wide-angle X-ray diffraction curves of native cellulose (spectrum a) and regenerated cellulose sample 3 (spectrum b). The diffraction curve of native cellulose is of typical cellulose I structure. It has strong crystalline peaks at  $14.8^\circ$ ,  $16.8^\circ$  and  $22.6^\circ$  corresponding to the (110), (1  $\bar{1}$  0), and (002) planes of crystals, and weak crystalline peaks at  $34.7^\circ$  to the (004) plane (Isogai, Usuda, Kato, Uryu, & Atalla, 1989; Oh et al., 2005). After dissolution and regeneration, the diffraction curve of regenerated cellulose sample 3 as well other curves of regenerated cellulose samples (curves not shown) are of the typical diffraction patterns of cellulose II by the presence of the broad crystalline peak at around  $19.8^\circ$  (Adinugraha, Marseno, & Haryadi, 2005; Isogai et al., 1989).

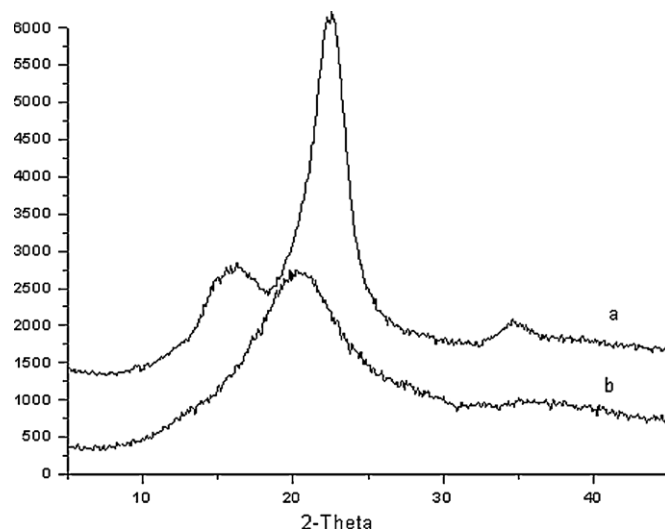


Fig. 4. Wide-angle X-ray diffraction curves of native cellulose (spectrum a) and regenerated cellulose sample 3 (spectrum b).

These results revealed that during dissolution and regeneration in  $[\text{C}_4\text{mim}]\text{Cl}$  assisted with ultrasound irradiation, the conversion of cellulose crystals from cellulose I in native cellulose to cellulose II in regenerated cellulose does occur. Similar results have been reported by Zhang et al. (2005) and Luo et al. (2005).

### 3.5. Thermal analysis

Fig. 5 shows the TGA curves of native cellulose (a) and regenerated cellulose samples 6 (b) and 10 (c). The small initial drops occurring near  $100^\circ\text{C}$  in all cases are due to the evaporation of retained moisture. A single pronounced decomposition followed by slow weight loss was observed in all curves. The native cellulose starts to decompose at  $228^\circ\text{C}$ , whereas the regenerated cellulose samples 6 and 10 begin to decompose at  $203^\circ\text{C}$  and  $228^\circ\text{C}$ , respectively. At 50% weight loss, the decomposition temperature occurs at  $338^\circ\text{C}$  for native cellulose,  $330^\circ\text{C}$  for regenerated cellulose sample 6, and  $285^\circ\text{C}$  for regenerated cellulose sample 10. These decreasing trends of decomposition temperature implied that the thermal stability of regenerated cellulose was lower than that of native cellulose. The reason of this decrement was probably due to partial hydrolysis and degradation of macromolecular cellulose during

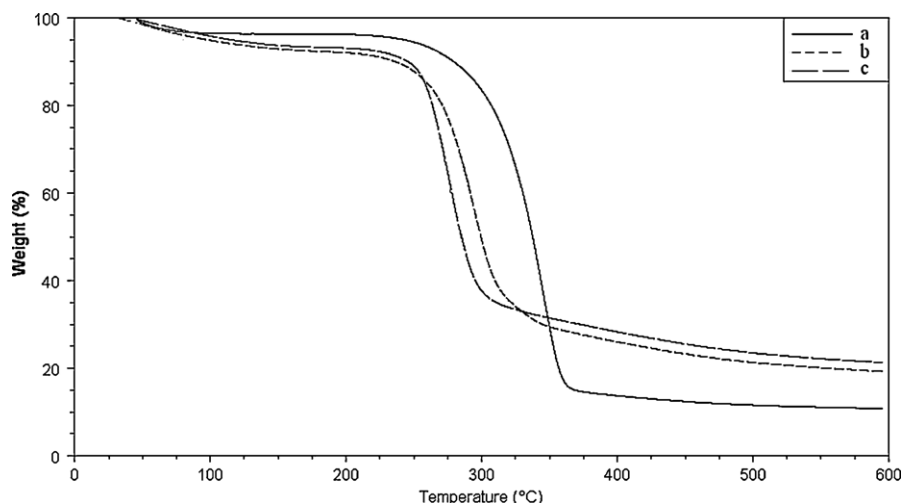


Fig. 5. TGA curves of native cellulose (a) and regenerated cellulose samples 6 (b) and 10 (c).

dissolution assisted with irradiation of ultrasound, especially with relatively high ultrasonic power. It was consistent with the present of absorbance at  $1574\text{ cm}^{-1}$  from anti-symmetric stretching of carboxylic anions in FT-IR spectrum of sample 10.

In addition, the residual char yields above  $600^\circ\text{C}$  were 11.5% for native cellulose, 18.6% for regenerated cellulose sample 6, and 21.2% regenerated cellulose sample 10. The similar decreased pyrolysis residues of regenerated cellulose after dissolution in ionic liquids were reported by Luo et al. (2005). Pyrolysis residues are primarily indecomposable inorganic salts. The higher pyrolysis residues of regenerated cellulose indicated that more inorganic salts were involved into cellulose after dissolution and regeneration in ionic liquids. This kind of inorganic salts could not be detected by the FT-IR and CP/MAS  $^{13}\text{C}$  NMR. It should be noted that the involvement of inorganic salts in regenerated cellulose samples would be the main reason of yield higher than 100%.

#### 4. Conclusion

Ultrasonic irradiation could effectively reduce the dissolution time of cellulose in ionic liquid  $[\text{C}_4\text{mim}]\text{Cl}$ . An increase of ultrasonic power from 20 to 50 W and irradiation time from 0 to 20 min resulted in the decrease in cellulose dissolution time. After dissolution and regeneration in ionic liquid, the crystalline structure of cellulose was converted from cellulose I to cellulose II. FT-IR, solid state CP/MAS  $^{13}\text{C}$  NMR and X-ray diffraction analyses indicated that the regenerated cellulose was a mixture of amorphous cellulose and cellulose II. The thermal stability of cellulose decreased and the pyrolysis residues increased after dissolution and regeneration in ionic liquid.

#### Acknowledgements

The authors are grateful for the financial support of this research from the National Natural Science Foundation of China (Nos. 30871994, 30972325, and 30710103906), the Guangdong Natural Science Foundation (No. 8451064101000409), Specialized Research Fund for the Doctoral Program of Higher Education (No. 20070561040), Chinese Universities Scientific Fund (No. 2009ZZ0024), and National Basic Research Program of China (No. 2010CB732201).

#### References

- Adewuyi, Y. G. (2001). Sonochemistry: Environmental science and engineering applications. *Industrial & Engineering Chemistry Research*, 40, 4681–4715.
- Adinugraha, M. P., Marseno, D. W., & Haryadi. (2005). Synthesis and characterization of sodium carboxymethylcellulose from cavendish banana pseudo stem (*Musa cavendishii* LAMBERT). *Carbohydrate Polymers*, 62, 164–169.
- Aliyu, M., & Hephher, M. J. (2000). Effects of ultrasound energy on degradation of cellulose material. *Ultrasonics Sonochemistry*, 7, 265–268.
- Araki, J., Kataoka, T., Katsuyama, N., Teramoto, A., Ito, K., & Abe, K. (2006). A preliminary study for fiber spinning of mixed solutions of polyrotaxane and cellulose in a dimethylacetamide/lithium chloride (DMAc/LiCl) solvent system. *Polymer*, 47, 8241–8246.
- Bardet, M., Foray, M. F., & Tran, Q. K. (2002). High-resolution solid-state CPMAS NMR study of archaeological woods. *Analytical Chemistry*, 74, 4386–4390.
- Biswas, A., Shogren, R. L., Stevenson, D. G., Willett, J. L., & Bhowmik, P. K. (2006). Ionic liquids as solvents for biopolymers: Acylation of starch and zein protein. *Carbohydrate Polymers*, 66, 546–550.
- Blakeney, A. B., Harris, P. J., Henry, R. J., & Stone, B. A. (1983). A simple and rapid preparation of alditol acetates for monosaccharide analysis. *Carbohydrate Research*, 113, 291–299.
- Chang, S. T., & Chang, H. T. (2001). Comparisons of the photostability of esterified wood. *Polymer Degradation and Stability*, 71, 261–266.
- de Maria, D., & Martinsson, A. (2009). Ionic-liquid-based method to determine the degree of esterification in cellulose fibers. *Analyst*, 134, 493–496.
- Evans, R., & Wallis, A. F. A. (1989). Cellulose molecular-weights determined by viscometry. *Journal of Applied Polymer Science*, 37, 2331–2340.
- Fischer, S., Leipner, H., Thummmler, K., Brendler, E., & Peters, J. (2003). Inorganic molten salts as solvents for cellulose. *Cellulose*, 10, 227–236.
- Forsyth, S. A., MacFarlane, D. R., Thomson, R. J., & von Itzstein, M. (2002). Rapid, clean, and mild O-acetylation of alcohols and carbohydrates in an ionic liquid. *Chemical Communications*, 7, 714–715.
- Fort, D. A., Remsing, R. C., Swatloski, R. P., Moyna, P., Moyna, G., & Rogers, R. D. (2007). Can ionic liquids dissolve wood? Processing and analysis of lignocellulosic materials with 1-n-butyl-3-methylimidazolium chloride. *Green Chemistry*, 9, 63–69.
- Fukaya, Y., Hayashi, K., Wada, M., & Ohno, H. (2008). Cellulose dissolution with polar ionic liquids under mild conditions: required factors for anions. *Green Chemistry*, 10, 44–46.
- Fukaya, Y., Sugimoto, A., & Ohno, H. (2006). Superior solubility of polysaccharides in low viscosity, polar, and halogen-free 1,3-dialkylimidazolium formates. *Biomacromolecules*, 7, 3295–3297.
- Heinze, T., Schwikal, K., & Barthel, S. (2005). Ionic liquids as reaction medium in cellulose functionalization. *Macromolecular Bioscience*, 5, 520–525.
- Hermanutz, F., Gaehr, F., Uerdingen, E., Meister, F., & Kosan, B. (2007). New developments in dissolving and processing of cellulose in ionic liquids. *Macromolecular Symposia*, 262, 23–27.
- Isogai, A., Usuda, M., Kato, T., Uryu, T., & Atalla, R. H. (1989). Solid-state CP/MAS carbon-13 NMR study of cellulose polymorphs. *Macromolecules*, 22, 3168–3172.
- Kamiya, N., Matsushita, Y., Hanaki, M., Nakashima, K., Narita, M., Goto, M., et al. (2008). Enzymatic in situ saccharification of cellulose in aqueous-ionic liquid media. *Biotechnology Letters*, 30, 1037–1040.
- Kardos, N., & Luche, J. L. (2001). Sonochemistry of carbohydrate compounds. *Carbohydrate Research*, 332, 115–131.
- Kilpelainen, I., Xie, H., King, A., Granstrom, M., Heikkinen, S., & Argyropoulos, D. S. (2007). Dissolution of wood in ionic liquids. *Journal of Agricultural and Food Chemistry*, 55, 9142–9148.
- Kosan, B., Michels, C., & Meister, F. (2008). Dissolution and forming of cellulose with ionic liquids. *Cellulose*, 15, 59–66.
- Liu, C. F., Sun, R. C., Zhang, A. P., Ren, J. L., Wang, X. A., Qin, M. H., et al. (2007). Homogeneous modification of sugarcane bagasse cellulose with succinic anhydride using an ionic liquid as reaction medium. *Carbohydrate Research*, 342, 919–926.
- Liu, C. F., Sun, R. C., Zhang, A. P., Qin, M. H., Ren, J. L., & Wang, X. A. (2007). Preparation and characterization of phthalated cellulose derivatives in room-temperature ionic liquid without catalysts. *Journal of Agricultural and Food Chemistry*, 55, 2399–2406.
- Liu, C. F., Zhang, A. P., Li, W. Y., Yue, F. X., & Sun, R. C. (2010). Succinylation of cellulose catalyzed with iodine in ionic liquid. *Industrial Crops and Products*, 31, 363–369.
- Luo, H. M., Li, Y. Q., & Zhou, C. R. (2005). Study on the dissolubility of the cellulose in the functionalized ionic liquid. *Polymeric Materials Science & Engineering*, 21, 233–235.
- Maunu, S. L. (2002). NMR studies of wood and wood products. *Progress in Nuclear Magnetic Resonance Spectroscopy*, 40, 151–174.
- Mazza, M., Catana, D. A., Vaca-Garcia, C., & Cecutti, C. (2009). Influence of water on the dissolution of cellulose in selected ionic liquids. *Cellulose*, 16, 207–215.
- Oh, S. Y., Yoo, D. I., Shin, Y., Kim, H. C., Kim, H. Y., Chung, Y. S., et al. (2005). Crystalline structure analysis of cellulose treated with sodium hydroxide and carbon dioxide by means of X-ray diffraction and FTIR spectroscopy. *Carbohydrate Research*, 340, 2376–2391.
- Philipp, B., Nehls, I., & Wagenknecht, W. (1987).  $^{13}\text{C}$ -NMR spectroscopic study of the homogeneous sulphation of cellulose and xylan in the  $\text{N}_2\text{O}_4$ -DMF system. *Carbohydrate Research*, 164, 107–116.
- Pu, Y. Q., Jiang, N., & Ragauskas, A. J. (2007). Ionic liquid as a green solvent for lignin. *Journal of Wood Chemistry and Technology*, 27, 23–33.
- Ramos, L. A., Frollini, E., & Heinze, T. (2005). Carboxymethylation of cellulose in the new solvent dimethyl sulfoxide/tetrabutylammonium fluoride. *Carbohydrate Polymers*, 60, 259–267.
- Ren, J. L., Sun, R. C., Liu, C. F., Cao, Z. N., & Luo, W. (2007). Acetylation of wheat straw hemicelluloses in ionic liquid using iodine as a catalyst. *Carbohydrate Polymers*, 70, 406–414.
- Rosenau, T., Hofinger, A., Potthast, A., & Kosma, P. (2003). On the conformation of the cellulose solvent N-methylmorpholine-N-oxide (NMMO) in solution. *Polymer*, 44, 6153–6158.
- Sun, X. F., Sun, R. C., Tomkinson, J., & Baird, M. S. (2004). Degradation of wheat straw lignin and hemicellulosic polymers by a totally chlorine-free method. *Polymer Degradation and Stability*, 83, 47–57.
- Swatloski, R. P., Spear, S. K., Holbrey, J. D., & Rogers, R. D. (2002). Dissolution of cellulose with ionic liquids. *Journal of the American Chemical Society*, 124, 4974–4975.
- Turner, M. B., Spear, S. K., Huddleston, J. G., Holbrey, J. D., & Rogers, R. D. (2003). Ionic liquid salt-induced inactivation and unfolding of cellulase from *Trichoderma reesei*. *Green Chemistry*, 5, 443–447.
- Xie, H., King, A., Kilpelainen, I., Granstrom, M., & Argyropoulos, D. S. (2007). Thorough chemical modification of wood-based lignocellulosic materials in ionic liquids. *Biomacromolecules*, 8, 3740–3748.
- Xie, H. B., Zhang, S. B., & Li, S. H. (2006). Chitin and chitosan dissolved in ionic liquids as reversible sorbents of  $\text{CO}_2$ . *Green Chemistry*, 8, 630–633.
- Zhang, H., Wu, J., Zhang, J., & He, J. S. (2005). 1-Allyl-3-methylimidazolium chloride room temperature ionic liquid: A new and powerful nonderivatizing solvent for cellulose. *Macromolecules*, 38, 8272–8277.